Journal of the European Ceramics Society 7 (1991) 295–305

Sol–Gel-Derived CaO- and CeO_2-stabilized ZrO_2 Fibers—Conversion Process of Gel to Oxide and Tensile Strength

Kanichi Kamiya, Kyoichi Takahashi, Takuya Maeda, Hiroyuki Nasu

Chemistry Department for Materials, Faculty of Engineering, Mie University,
Kamihama, Tsu, Mie-ken 514, Japan

&

Toshinobu Yoko

Institute for Chemical Research, Kyoto University, Gokasho, Uji, Kyoto-fu 611, Japan

(Received 4 October 1990; revised version received 18 December 1990; accepted 21 December 1990)

Abstract

The $11CaO.89ZrO_2$ *(in mol%) fibers were fabricated by the sol–gel method using* $Zr(O\text{-n-}C_3H_7)_4$ *and* $Ca(CH_3COO)_2.H_2O$ *or* $Ca(NO_3)_2.4H_2O$*. The maximum tensile strength of 1000°C-treated fibers was 0·8–1·0 GPa at diameters of 10–15 μm. However, the strength of the alkoxide/acetate-derived fibers decreased with increasing diameter at a greater rate than that of the alkoxide/nitrate-derived fibers. This was associated with the sudden removal of acetate groups at a unique temperature, and was explained by the increased difficulty in the removal of acetate groups through the oxide matrix without forming microcracks in the fibres having increased diameters.*

For the CeO_2–ZrO_2 *fibers made from* $Zr(O\text{-n-}C_3H_7)_4$ *and* $Ce(NO_3)_3.6H_2O$*, a maximum tensile strength of 1·0–1·2 GPa was attained at diameters of 10–15 μm. The addition of a small amount of CuO as a sintering aid much improved the mechanical properties of the fibers, resulting in fibers with tensile strength as high as 1·8–2·0 GPa.*

Über das Sol–Gel Verfahren wurden aus $Zr(O\text{-n-}C_3H_7)_4$ *und* $Ca(CH_3COO)_2.H_2O$ *oder* $Ca(NO_3)_2.4H_2O$ *Fasern mit der Zusammensetzung* $11CaO.89ZrO_2$ *(Mol.%) hergestellt. Fasern, die bei 1000°C kalziniert wurden, hatten bei Durchmessern von 10 μm bis 15 μm eine maximale Zugfestigkeit von 0·8–1·0 GPa. Bei zunehmendem Radius zeigte sich jedoch bei den Fasern aus der Alkoxid/Acetat-Mischung eine stärkere Festigkeitsabnahme als bei den Fasern aus der Alkoxid/Nitrat-Mischung. Dies wurde darauf zurückgeführt, daß die Acetatgruppen bei einer bestimmten Temperatur spontan entweichen. Ferner wird das Entweichen der Acetatgruppen mit zunehmendem Durchmesser durch die oxidische Matrix ohne Mikrorißbildung immer schwieriger. Des weiteren wurden aus* $Zr(O\text{-n-}C_3H_7)_4$ *und* $Ce(NO_3)_3.6H_2O$ CeO_2–ZrO_2 *Fasern hergestellt, die bei Durchmessern von 10 μm 15 μm eine maximale Zugfestigkeit von 1·0–1·2 GPa aufwiesen. Eine geringfügige Zugabe von CuO als Sinterhilfsmittel konnte die mechanischen Eigenschaften der Fasern stark verbessern. Diese Fasern zeigten Zugfestigkeiten von bis zu 1·8–2·0 GPa.*

On a préparé des fibres $11CaO.89ZrO_2$ *(% molaires) par la méthode sol–gel, en utilisant* $Zr(O\text{-n-}C_3H_7)_4$ *et* $Ca(CH_3COO)_2.H_2O$ *ou* $Ca(NO_3)_2.4H_2O$*. La résistance maximale à la traction de fibres de diamètre compris entre 10 et 15 μm, traitées à 1000°C, était de 0·8–1·0 GPa. La décroissance de la résistance avec le diamètre était plus prononçée dans le cas des fibres issues de la composition alcoolate/acétate que dans celui des fibres élaborées à partir de la composition alcoolate/nitrate. Cet effet était associé au départ brusque des groupes acétate à une température particulière et a été expliqué par le fait que l'élimination des groupes acétates à travers la matrice oxyde sans formation de microfissures est rendue plus difficile pour des fibres possédant un diamètre élevé. Pour les fibres* CeO_2–ZrO_2 *obtenues à partir de* $Zr(O\text{-n-}C_3H_7)_4$ *et* $Ce(NO_3)_3.6H_2O$*, une* *résistance maximale à la traction de 1·0–1·2 GPa a été atteinte pour des diamètres de 10 à 15 μm. L'ajout, en faible quantité, de CuO comme dopant de frittage permet d'élever de manière sensible les propriétés mécaniques de ces fibres, la résistance à la traction atteignant 1·8–2·0 GPa.*

Introduction

Ceramic fibers have been fabricated for lightweight refractory packing, and high-strength ones have been made for the reinforcement of ceramics and metals. Stabilized ZrO_2 fibers with high mechanical strength have attracted much attention because of their high mechanical toughness as well as their high refractoriness.

Commercially available zirconia fibers have been produced through a somewhat complicated method, in which porous organic polymer fibers are impregnated with an aqueous zirconium salt such as $ZrOCl_2$ and then oxidized by heat-treating in air. The mechanical strength of the fibers, however, is not high enough for application in fiber-reinforced composites.

Y_2O_3-stabilized ZrO_2 fibers, which have diameters in the range 2 to 5 μm and tensile strength in the range 1·5 to 2·6 GPa, have been produced by spinning the concentrated and viscous sols consisting of zirconium acetate and yittrium nitrate and then heating the drawn fibers to ~1400°C.[1,2]

The present authors[3,4] have been investigating the sol–gel method for preparing oxide glass and/or ceramic fibers, in which metal alkoxides are partially hydrolyzed with a limited amount of water to produce linear-type metalloxane polymers suitable for fiber-drawing. Previously, the sol–gel method was applied to the fabrication of CaO-stabilized ZrO_2 fibers using $Zr(O\text{-}n\text{-}C_3H_7)_4$ and $Ca(CH_3COO)_2 . H_2O$ as raw materials, and reaction conditions for making spinnable sols and some preliminary results on the conversion process of gel fibers to oxide fibers were reported.[5,6] Since then, several modifications of the alkoxide-method for making zirconia fibers have been reported,[7,8] in which the functionality of zirconium alkoxide is reduced from 4 to 2–3 by forming complexes with chelating reagents such as acetylacetone, in order for the hydrolysis–condensation of the alkoxide to proceed unidirectionally and to achieve stable spinning. However, the effect of the chelation of the starting alkoxide on the properties of resultant fibers has not been reported.

Moreover, so far, Y_2O_3-stabilized ZrO_2 fibers have been extensively investigated because of their good mechanical properties. However, Y_2O_3–ZrO_2 ceramics undergo low-temperature moisture degradation.[9] CeO_2–ZrO_2 fibers[10] are being developed as an alternative to Y_2O_3–ZrO_2 fibers because of their higher resistivity against moisture.[11] It seems interesting, therefore, to produce CeO_2–ZrO_2 fibers for mechanical application.

In the present work fibers of the CaO–ZrO_2 system were first fabricated using $Zr(O\text{-}n\text{-}C_3H_7)_4$ and different CaO sources, and the conversion process of gel to oxide fibers and tensile strength of fibers were compared with each other. Then, on the basis of the results for the CaO–ZrO_2 fibers, CeO_2–ZrO_2 fibers were made by the sol–gel method and their tensile strength was measured.

2 Experimental

2.1 CaO–ZrO_2 fibers

2.1.1 Preparation of fibers

$Zr(O\text{-}n\text{-}C_3H_7)_4$ (Alpha Products) and reagent grade $Ca(CH_3COO)_2 . H_2O$ or $Ca(NO_3)_2 . 4H_2O$ were used as raw materials. $Zr(O\text{-}n\text{-}C_3H_7)_4$ (22·4 g) was dissolved in 63·3 g anhydrous ethanol. The ethanolic solution of 1·17 g $Ca(CH_3COO)_2 . H_2O$ or 1·53 g $Ca(NO_3)_2 . 4H_2O$ containing aqueous hydrochloric acid was added dropwise to the alkoxide solution using a burette under stirring at room temperature (20–25°C). Hydrochloric acid acted as a peptizing agent. The composition of the starting solution of $Zr(O\text{-}n\text{-}C_3H_7)_4$–$Ca(CH_3COO)_2$ or $Ca(NO_3)_2$–H_2O–C_2H_5OH–HCl was in the spinnable region,[5] namely, the molar ratio of water which comes from the CaO source and hydrochloric acid was unity to the sum of metal sources, and that of C_2H_5OH and HCl was 25·0 and 0·3, respectively. The amounts of $Zr(O\text{-}n\text{-}C_3H_7)_4$ and the CaO source correspond to the analyzed composition of 11CaO . 89ZrO_2 (in mol%). In the following sections, alkoxide/acetate- and alkoxide/nitrate-derived CaO–ZrO_2 compositions are abbreviated as 11C(A) and 11C(N), respectively.

The mixed alkoxide solution thus prepared was heated to 80°C without any covers. When the solution became viscous and showed a little spinnability (within 1·5 to 2 h), it was cooled to room temperature for spinning. The fiber-drawing was conducted by immersing a glass rod into the viscous sol and pulling it up by hand. The hand-drawn gel fibers were 20 to 50 cm in length and from ~10 μm to several tens μm in diameter. No significant difference in the 80°C-aging time required for the solution to attain viscous state and spinnability between solutions for 11C(A) and 11C(N) was observed.

The gel fibers dried in the room for weeks were heated in air with a heating rate of 5°C/min and held at the desired temperatures for 1 h, and were subjected to infrared (IR), X-ray diffraction (XRD), pore characteristics and scanning electron microscope (SEM) measurements.

2.1.2 Measurements

Infrared spectra of fibers heated to different temperatures were obtained in the range from 400 to 4000 cm^{-1} using an IR spectrometer A-202 (Nihon Bunko Co., Japan). For that purpose, a small amount of pulverized specimen was mixed with KBr powders, and pressed into a pellet.

The X-ray diffraction technique was adapted for the identification of crystalline species precipitating in the heated fibers. The crystallite size of the tetragonal ZrO_2, if any, was determined on the basis of line-broadening of the (101) line. In the case of coexistence of monoclinic ZrO_2 (m-ZrO_2) with tetragonal ZrO_2 (t-ZrO_2) in fibers, the fraction of t-ZrO_2 (T%) was estimated from the diffraction intensities of respective ZrO_2 phases by use of the following equation:

$$\mathrm{T}(\%) = \frac{I_{\mathrm{T}(101)}}{I_{\mathrm{M}(111)} + I_{\mathrm{M}(111)} + I_{\mathrm{T}(101)}}$$

where $I_{\mathrm{T}(101)}$, $I_{\mathrm{M}(111)}$ and $I_{\mathrm{M}(111)}$ denote the diffraction intensity of the (101) line of t-ZrO_2, (111) and (111) lines of m-ZrO_2, respectively.

Pore characteristics (surface area, micropore volume and mean pore radius) were measured with a Sorptmatic 1800 (Carlo Erba Co.) by the absorption and desorption of nitrogen gas. All samples were vacuum-dried at 150°C before measurements.

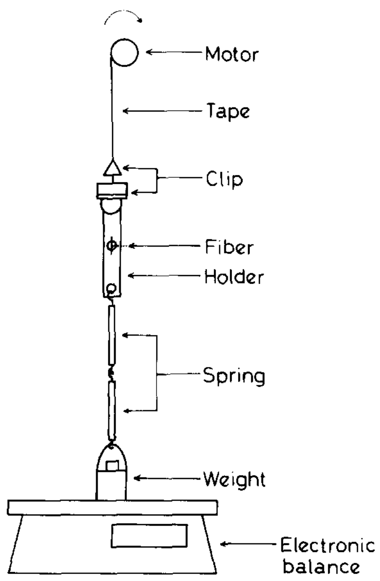

Fig. 1. A set-up for measurement of tensile strength of a single fiber.

DTA/TG analyses were made for gel fibers using a machine TAS-100 (Rigaku Co.) under air and/or in a N_2 atmosphere. A heating rate of 5°C/min was used.

The tensile strength of zirconia fibers was measured using a laboratory-made set-up which is schematically shown in Fig. 1. A single fiber was set to a reactangular paper (60 mm × 100 mm) with organic adhesive across a 2 mm diameter hole bored at center. After setting to the machine, the paper was cut off at both sides of the hole, and tensile stress was applied by pulling up the fiber together with an attached weight put on the electric balance. The loading velocity was 0·1 g/s. Fracture-load was read from the balance and converted to tensile strength by dividing by cross-sectional area which was measured under an optical microscope.

2.2 CeO_2–ZrO_2 fibers

The $Zr(O\text{-}n\text{-}C_3H_7)_4/Ce(NO_3)_3$–$H_2O$–$C_2H_5OH$–HCl solutions were prepared in a similar manner to that used in Section 2.1.1. Raw materials were weighed so that the analyzed composition of the resultant fibers was $10CeO_2.90ZrO_2$ or $19CeO_2.81ZrO_2$ (in mol%). Hereafter, these compositions are abbreviated as 10 E(N) and 19E(N), respectively. To the latter composition CuO was added as a sintering aid in amounts of 1·0 and 3·0 mol% (for that purpose, a prescribed amount of $Cu(NO_3)_2.3H_2O$ was added to the starting solution). The fibers drawn from 80°C-aged solutions by hand and heated to various temperatures in air were subjected to XRD, SEM observation and tensile strength measurement.

3 Results

3.1 CaO–ZrO_2 fibers

3.1.1 IR spectra of fibers

IR spectra of 11C(A) fibers heated to different temperatures are shown in Fig. 2a together with that of $Ca(CH_3COO)_2.H_2O$. A broad absorption peak around 3500 cm^{-1} is ascribed to water included in the samples and/or absorbed in the KBr pellet. Absorption peaks characteristic to acetate groups are found in the range 1300 to 1600 cm^{-1} (COO) and at 1050 cm^{-1} (—CH_3), ~1000 cm^{-1} (CH_3) and 650 cm^{-1} (COO). A 1630 cm^{-1} peak is for water and/or C = O groups.

It has been known that a peak around 1400 cm^{-1} is split into two or more peaks, as is seen in the

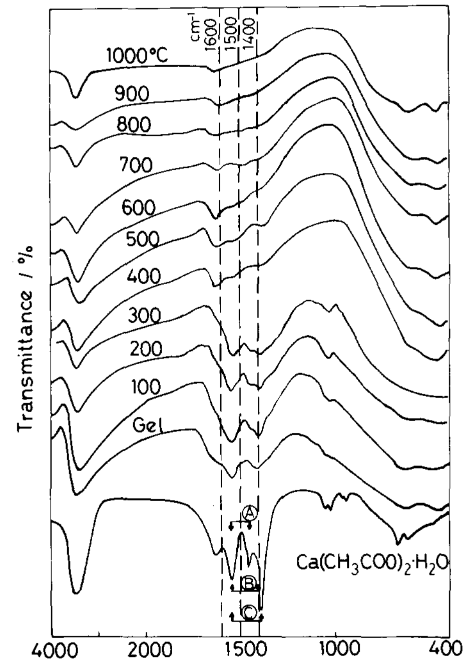

Fig. 2a. IR spectra of Ca$(CH_3COO)_2 . H_2O$ and alkoxide/acetate-derived 11CaO.89ZrO$_2$ (in mol%) (11C(A)) fibers heated to indicated temperatures (for A, B and C, see text).

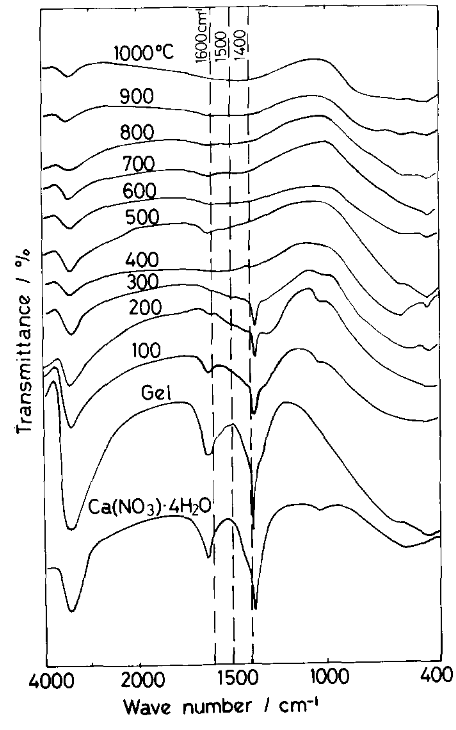

Fig. 2b. IR spectra of Ca$(NO_3)_2 . 4H_2O$ and alkoxide/nitrate-derived 11CaO.89ZrO$_2$ (in mol%) (11C(N)) fibers heated to the indicated temperatures.

spectrum of Ca$(CH_3COO)_2 . H_2O$, depending on surroundings of the acetate group.[12] As indicated by arrows in the figure, a set of peaks A (1550 and 1450 cm^{-1}) may correspond to acetate group **I** (monodentate), set B (1550 and 1420 cm^{-1}) to an ionic acetate and set C (1550 and 1390 cm^{-1}) to chelating (**II**) or bridging (**III**) acetate group.

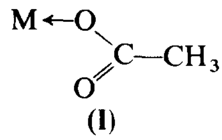
(I)

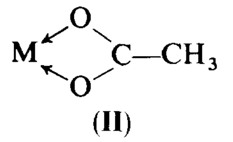
(II)

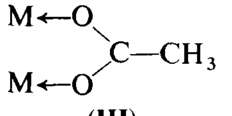
(III)

The IR spectrum of 11C(A) gel fibers is very similar to that of Ca$(CH_3COO)_2 . H_2O$ except in the wavenumber range lower than 600 cm^{-1}, although peaks are somewhat broadened. Peaks in the range 1400 to 1600 cm^{-1} indicate that acetate groups in gel fibers are present as monodentate, ionic, chelating and/or bridging groups (a large proportion of the acetate groups is covalently bonded to metals). A very broad band at a low wavenumber range, which becomes stronger on increasing heating temperature, is attributed to Zr—O bonds.

At 400°C, a considerable amount of the acetate groups is removed from gel, leaving some more tightly bonded groups. A growth of the 1630 cm^{-1} peak at this temperature may indicate the formation of carbonate groups due to oxidation of acetate groups. The decrease in intensity of the 1400–1600 cm^{-1} peaks is continued to 1000°C.

In Fig. 2b, the variation of the IR spectrum of 11C(N) fibers with heating temperature is shown. The spectrum of Ca$(NO_3)_2 . 4H_2O$ is also shown as a reference. IR peaks around 3500 and 1630 cm^{-1} in Ca$(NO_3)^2 . 4H_2O$ are for water. A sharp peak at 1390 cm^{-1} and a small one around 1050 cm^{-1} are ascribed to isolated NO_3^- ions. Shoulders on both sides of the 1390 cm^{-1} peak are for NO_3^- groups covalently bonded to metal atoms in forms such as monodentate, chelating and bridging.

The IR spectrum of the gel suggests that NO_3^- groups are incorporated into the gel in a similar fashion to Ca$(NO_3)_2 . 4H_2O$, namely, a majority of NO_3^- groups is present in an ionic state in the gel. At 400°C, the 1390 cm^{-1} peak disappears, but a broad band attributable to covalently bonded NO_3^- groups remains, the latter being scarcely observed above 700°C.

In Figs 2a and 2b, no peaks ascribable to alkoxy group (—O-*n*-C_3H_7) are observed, which implies that alkoxy groups remaining unreacted in the sol state are almost completely removed during drying of gels in the room due to hydrolysis by air-moisture.

3.1.2 Crystallization behavior of gel fibers

Both gels started to crystallize at 400°C. The crystalline species precipitating first was c-ZrO_2 (cubic) or t-ZrO_2. The species observed at higher temperature was identified as t-ZrO_2. A proportion of t-ZrO_2 was transformed at 1000°C.

3.1.3 Pore characteristics of fibers

Pore-size distribution curves of 11C(A) and 11C(N) fibers heated to various temperatures are shown in Figs 3a and 3b. In Fig. 4, both the surface area and pore volume of fibers are shown as a function of heating temperature. Measurement was made twice and the average value was plotted. All the data except one for surface area at 500°C fall within the marks. It is seen that surface area is increased above 200°C and then begins to decrease at 500–600°C. The variation of pore volume seems two-step, that is, two maxima appear around 500 and 800°C. The 11C(N) fibers have a maximum surface area at a temperature higher by about 100°C than 11C(A) fibers. The pore volume of 11C(N) fibers is smaller than that of 11C(A) fibers at any temperature in the range where a large change in pore structure occurs. A significant difference in the pore-size distribution between 800°C-treated 11C(A) and 11C(N) fibers is noticed, that is, there is not only a larger pore volume but also a considerably larger mean pore radius in the former than the latter.

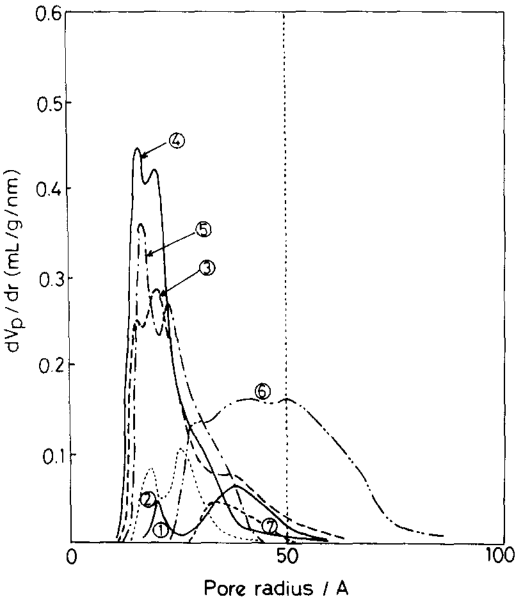

Fig. 3a. Pore size distribution curves for 11C(A) fibers heated to different temperatures, Gel dried at ① 150°C, ② 200°C ③ 400°C, ④ 500°C, ⑤ 600°C, ⑥ 800°C, ⑦ 1000°C.

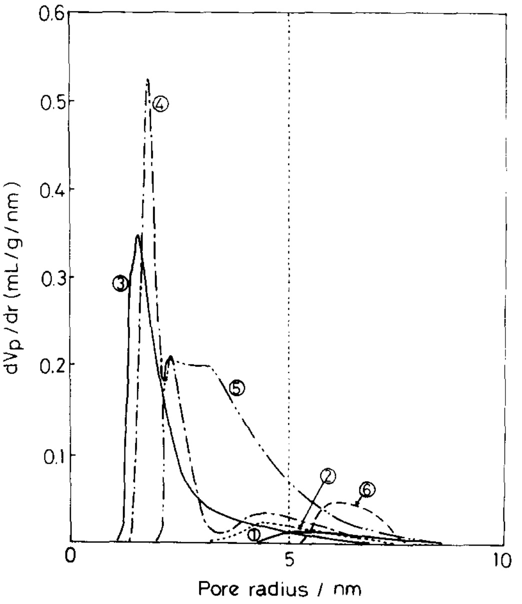

Fig. 3b. Pore size distribution curves for 11C(N) fibers heated to different temperatures. Gel dried at ① 150°C, ② 200°C, ③ 500°C, ④ 600°C, ⑤ 800°C, ⑥ 1000°C.

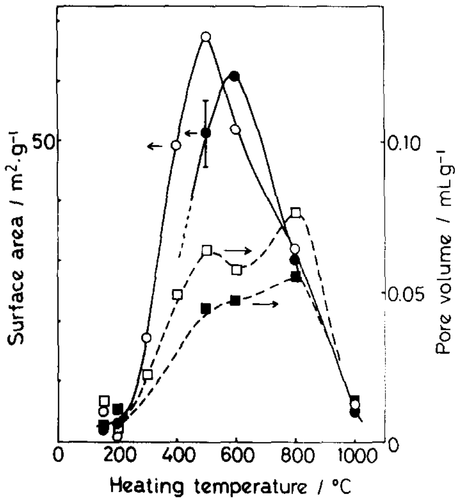

Fig. 4. Surface area and pore volume of 11CaO.89ZrO_2 (in mol%) fibers plotted as a function of heating temperature. ○ and ●, surface area; □ and ■, pore volume. Open and closed symbols represent 11C(A) and 11C(N) fibers, respectively.

3.1.4 Results of thermal analyses

DTA and TG curves of 11C(A) and 11C(N) fibers are shown in Fig. 5. A large weight loss and an endothermic peak observed below 150°C are due to

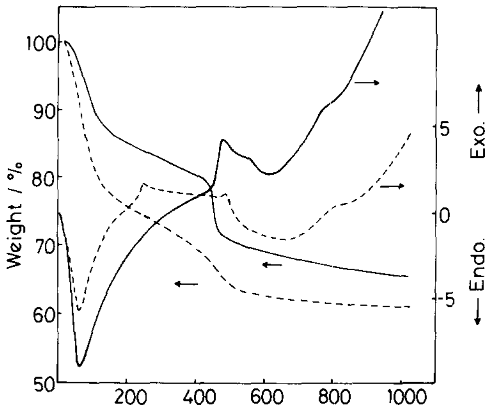

Fig. 5. DTA-TG curves of gel fibers for 11C(A) (———) and 11C(N) (- - - -).

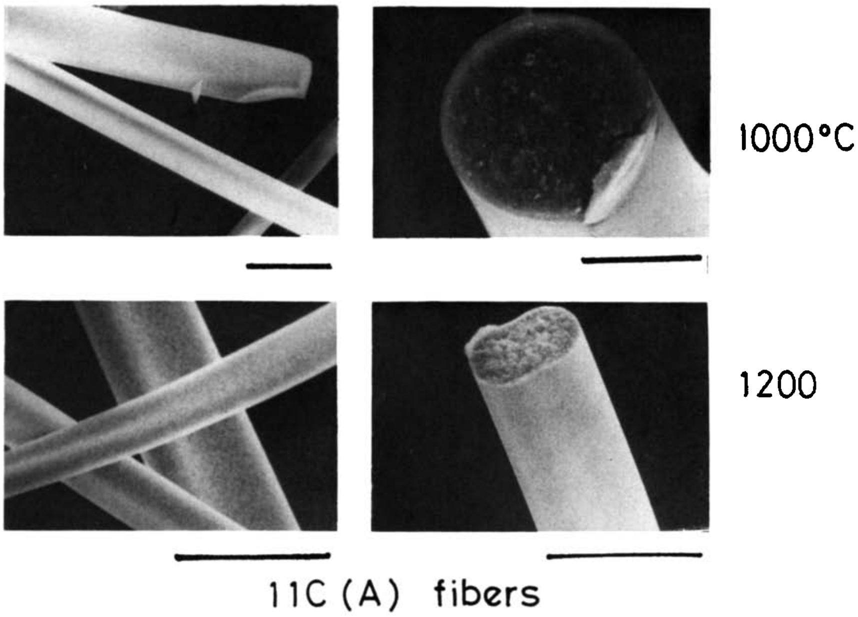

(a)

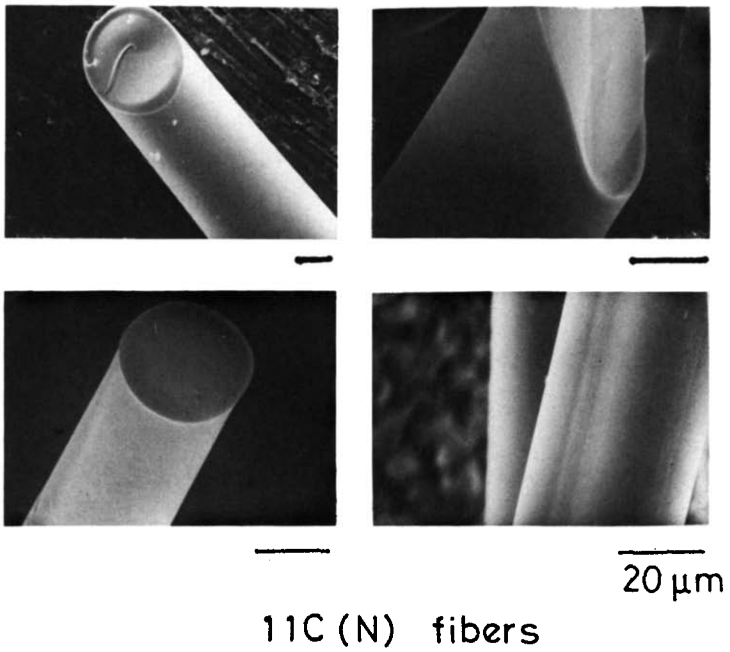

(b)

Fig. 6. SEM photographs of (a) 11C(A) and (b) 11C(N) fibers heat-treated at the indicated temperatures. (Bar is 20 μm in each case.)

the evaporation of alcohol remaining in the gel and absorbed water. The 11C(A) exhibits a sudden weight loss accompanied by a complex exothermic peak at 450°C, followed by gradual weight loss lasting to 1000°C. The sudden decrease in weight was also observed at 450°C under the N_2 atmosphere.

On the other hand, 11C(N) shows a rather gradual loss of weight in the temperature range 400 to 500°C. The decrease of weight is almost stopped at 800°C. Furthermore, two small exothermic peaks appear at 250°C and 500°C.

In both fibers, a faint and broad exothermic peak is observable around 800°C.

3.1.5 SEM observation

The heat-treated 11C(A) fibers have a smooth appearance at the fiber surface but a somewhat coarse texture at the core even at 1000°C as seen in the SEM photographs in Fig. 6, while 1000°C- and 1100°C-treated 11C(N) fibers are smooth at the fiber surface and the fracture surface.

3.1.6 Tensile strength of fibers

Tensile strength of 11C(A) and 11C(N) fibers heated to 1000°C under ambient atmosphere was measured. The fraction of t-ZrO_2 in the 11C(A) and 11C(N) fibers was 97 and 94%, respectively, and the

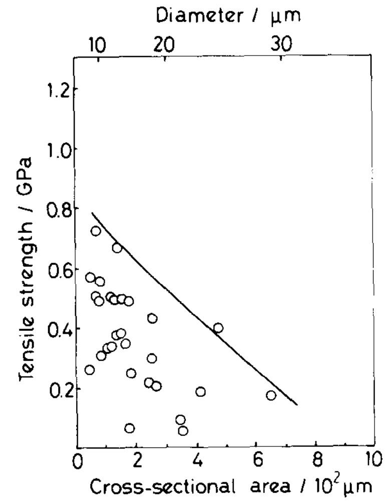

Fig. 7. Tensile strength of 1000°C-treated 11C(A) fibers plotted against cross-sectional area (or diameter). The solid line is an envelope of datum points.

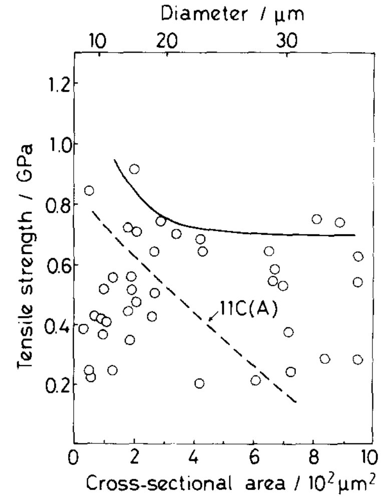

Fig. 8. Tensile strength of 1000°C-treated 11C(N) fibers plotted against cross-sectional area (or diameter). The broken line is the envelope for 1000°C-treated 11C(A) fibers.

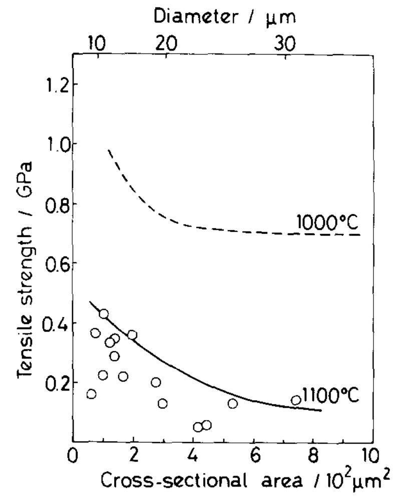

Fig. 9. Tensile strength of 1100°C-treated 11C(N) fibers plotted against cross-sectional area (or diameter). The broken line is the envelope for 1000°C-treated 11C(N) fibers.

crystallite size of t-ZrO_2 was 26–27 nm in both specimens.

Since hand-drawn fibers do not have a constant diameter and a unique shape in cross-section, the tensile strength of fibers is plotted against cross-sectional areas, as in Figs 7–9. As is seen, strength data are scattered, which may be caused by several factors acting to decrease the strength, such as difference in the smoothness of fiber surface, twisting of fibers and accidental torsion during measurement by which a fiber may be subjected to shear stress rather than tensile stress. Namely, it cannot be necessarily stated that all of the data have the same physical meaning, making difficult the statistical treatment of strength data. Furthermore, tensile strength of fibers should depend on fiber diameter.[13] Therefore, in the present work, a curve running through the maximum strength values at different cross-sectional areas is used to represent the strength of fibres. The curve was drawn freehand, taking the error of 5–10% (increasing with the decrease of cross-sectional area) in cross-sectional area and correspondingly in tensile strength of fibers into account.

The tensile strength of 1000°C-treated 11C(A) fibers (Fig. 7) is about 0·7 GPa at a cross-sectional area of 80 μm^2 (corresponding to 10 µm of diameter of a fiber with a round cross-section). The tensile strength is rapidly decreased with the increase of cross-sectional area or fiber diameter. The heat-treatment under the N_2 atmosphere and slower heating in the temperature range 400 to 500°C did not have any effect on strength of the fibers.

The 1000°C-treated 11C(N) fibers have a slightly higher tensile strength than 11C(A) fibers at a cross-sectional area of 200 μm^2 (diameter of ~ 15 µm) (Fig. 8). Furthermore, in contrast to 11C(A) fibers, a small diameter dependence of tensile strength is seen. The 11C(N) fibers decreased in strength with heating to 1100°C, as is shown in Fig. 9. The 1200°C-treated ones were too fragile for the strength to be measured.

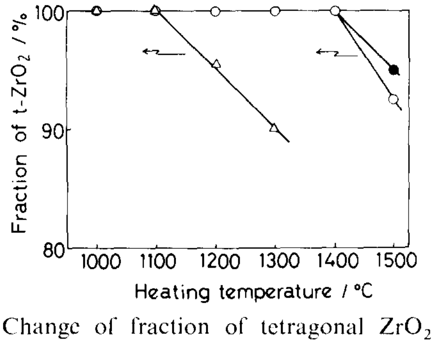

Fig. 10. Change of fraction of tetragonal ZrO_2 phase in alkoxide/nitrate derived CeO_2–ZrO_2 fibers with heating temperature. △, 10E(N), ○, 19E(N), ●, 1 mol% CuO–19E(N).

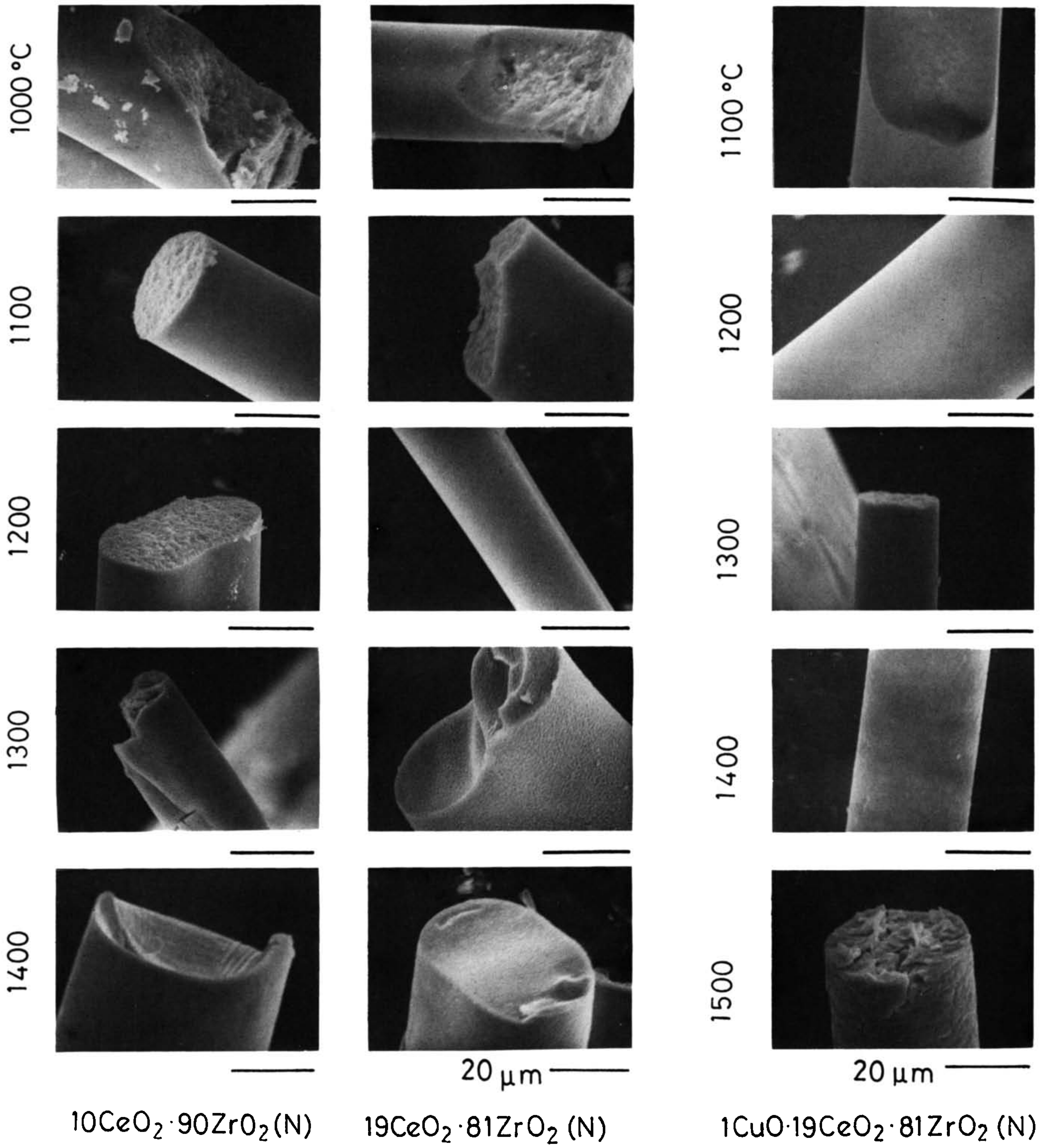

(a) (b) (c)

Fig. 11. SEM photographs of CeO_2–ZrO_2 fibers heated to the indicated temperatures. (a) 10E(N); (b) 19E(N); (c) 1 mol% CuO–19E(N). (Bar is 20 µm in each case.)

3.2 CeO_2–ZrO_2 fibers

The alkoxide/nitrate-derived CeO_2–ZrO_2 fibers, that is, 10E(N) and 19E(N) fibers, released ionically bonded NO_3^- groups gradually around 400°C, crystallizing into t-ZrO_2. The variation of the fraction of t-ZrO_2 in the fibers with heating temperature is shown in Fig. 10. In 10E(N) fibers a small portion of t-ZrO_2 is transformed to m-ZrO_2 above 1200°C, while t-ZrO_2 lasts to 1400°C in 19E(N) fibers. The addition of a sintering aid (CuO) at 1·0 mol% caused no significant change in the crystallization behavior of fibers. However, the addition of 3 mol% CuO gave rise to the precipitation of CeO_2 above 900°C and degraded fibers.

Figure 11(a), (b) and (c) shows SEM photographs of 10E(N), 19E(N), and 1·0 mol% CuO-containing

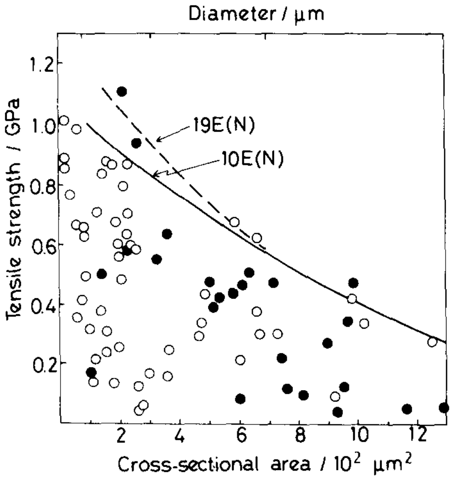

Fig. 12. Tensile strength of 1000 C-treated CeO_2-ZrO_2 fibers plotted against cross-sectional area. ○, 10E(N); ●, 19E(N). The solid line is an envelope for 10E(N) and the broken line is for 19E(N).

19E(N) fibers, respectively, heated to different temperatures. In 10E(N) and 19E(N) fibers, coarsening of grains is observed at 1200°C. The addition of CuO to 19E(N) fibers seems to suppress the grain growth, as seen in Fig. 11(c). At 1500°C, however, grain growth accompanied by crack formation is encountered.

The tensile strength of 10E(N) and 19E(N) fibers heated to 1000°C in air is plotted against cross-sectional area in Fig. 12. The maximum strength of about 1·0 GPa is attained in the 10E(N) fibers. It seems that the 19E(N) fiber is slightly stronger than 10E(N). As shown in Fig. 13, the addition of 1·0 mol% CuO has much improved the tensile strength, and 19E(N) fibers with CuO added show strength as high as 1·8–2·0 GPa at diameters of ~ 10 μm. The strength goes down at higher temperature, as can be seen from strength curves for CuO-containing fibers heated to different temperatures.

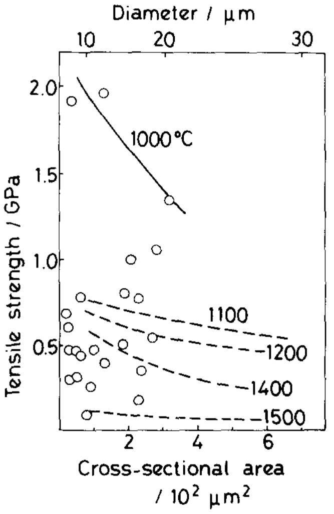

Fig. 13. Tensile strength of 1000°C-treated 1 mol% CuO–19E(N) fibers plotted against cross-sectional area. The broken lines are envelopes for the fibers heated to the indicated temperatures.

4 Discussion

4.1 Difference in thermal evolution between alkoxide/acetate- and alkoxide/nitrate-derived CaO–ZrO_2 gel fibers

As has been stated in Section 3, no noticeable difference in the reaction time needed for the occurrence of spinnability and fiber-drawing behavior between starting solutions for 11C(A) and 11C(N) was observed.

As to the thermal evolution of gel fibers, in a rough sense, two important structural changes occur during heating in both compositions. The first one occurs at 400–500°C, where a large portion of the acetate or NO_3^- groups incorporated into gel structure is thermally removed, leaving micropores, and at the same time, c- or t-ZrO_2 is precipitated in the fibers. A small exothermic peak at 400–500°C associated with a large weight loss is attributed to the crystallization of gel fibers.

The second important thermal change is one which occurs around 800°C. XRD, IR and TG measurements could not detect this evolution, but a small and broad exothermic peak in the DTA curve and an increase in the pore volume and mean pore radius was observed around 800°C. Pore characteristics data suggest that pores formed on removal of acetate or NO_3^- groups at 400–500°C coalesce into larger ones at 800°C, and heating at higher temperatures leads to sintering of fibers. A broad exothermic peak around 800°C may correspond to such a rearrangement of micropores or initiation of sintering (which should release surplus surface energy).

These roughly summarized observations are common to 11C(A) and 11C(N) fibers. However, the following difference in thermal evolution between the two fiber samples may be observed, which may originate from the difference in CaO-source.

The acetate groups, the majority of which are incorporated into 11C(A) fibers to form chelating or bridging bonds (covalent bond) with Ca or Zr atoms, are suddenly removed at 450°C in air. The combustion of removed acetate groups gives rise to a broad exothermic peak in the DTA curve which is overlapped with a sharp peak associated with crystallization. At the same time, carbonate groups are formed and incorporated into the gel structure, giving a small IR peak at 1630 cm^{-1}. The decomposition of carbonate groups and the remaining more tightly bonded acetate groups last up to 1000°C, which is confirmed by IR and TG measurements.

On the other hand, the removal of NO_3^- groups from 11C(N) fibers is rather sluggish and occurs in the somewhat wider temperature range of 350 to 550°C, compared to 11C(A) fibers. The removal of NO_3^- is accompanied by nothing other than crystallization and micropore formation. Furthermore, the removal of the remaining more tightly bonded NO_3^- is almost stopped at a lower temperature than acetate groups.

The difference in pore structure, namely the difference in mean pore radius, surface area and pore volume, may be ascribed to the difference in size between NO_3^- and acetate groups, of which sizes were estimated based on the atomic distances and atomic (or ionic) radii to be 0·52 and 0·57 nm, respectively. The 100°C higher peaking in the surface area–temperature curve for 11C(N) fibers may be due to less abrupt removal of NO_3^- ions than acetate groups.

4.2 Relation between thermal conversion process and tensile strength of fibers

The similar maximum tensile strength (0·8–0·9 GPa) was achieved in both 1000°C-treated 11C(A) and 11C(N) fibers of small cross-sectional area of $\sim 100\,\mu m^2$ (or diameters of 10–15 μm). However, 11C(A) fibers showed a larger cross-sectional area (or diameter) dependence of tensile strength than 11C(N) fibers. In general, the decrease of tensile strength of fibrous materials with the increase of fiber diameter has been explained by the increased probability to meet microflaws on increasing fiber diameter.

Among several structure changes in fibers encountered during heating, the removal of acetate or NO_3^- groups to leave micropores may be an important one affecting the mechanical properties of the resultant fibers. The sudden removal of acetate groups at a unique temperature may damage the fibers, while that of NO_3^- may not be so serious because of its smaller size (even though it is only a little smaller) and weak bonding (ionic) to gel matrix. As long as the fiber diameter is small, this is not the case even in 11C(A) fibers, because the path for gaseous decomposition products to be transported through the oxide matrix is short. However, when the fiber diameter is increased, it becomes difficult for gaseous products to get out of the fiber matrix without forming failures in fibers. In this case, it is considered that damage cannot be healed completely at 1000°C, leaving many microflaws on the fiber surface.

The 11C(A) fibers heated to 1000°C under N_2 atmosphere were as strong as those heated in air and showed a similar diameter dependence of tensile strength. This fact implies that the combustion of acetate groups in air may occur at the surface of fibers and scarcely affect the mechanical strength of resultant fibers.

In conclusion, calcium nitrate seems to be a better source for CaO than calcium acetate for obtaining CaO-stabilized ZrO_2 fibers with high tensile strength. Alkoxy groups did not seem to affect the conversion process of gel to oxide fibers and tensile strength of resultant fibers, because they are almost completely removed during drying of gels under ambient conditions through hydrolysis by humidity.

4.3 CeO_2–ZrO_2 fibers and the effect of CuO addition on their tensile strength

The maximum tensile strength attained in the alkoxide/nitrate-derived CeO_2–ZrO_2 fibers (10E(N) and 19E(N)) was 1·0–1·2 GPa at diameters of 10–15 μm. The addition of a small amount of CuO to 19E(N) fibers was very effective in increasing the tensile strength, namely, 1000°C-treated fibers became about two times stronger (1·8–2·0 GPa) by adding 1·0 mol% CuO, and the strength of 1100–1200°C-treated fibers containing CuO was still as high as 0·7–0·8 GPa at 10–15 μm in diameter, while that of fibers without CuO went down to ~0·5 GPa at 1100–1200°C. The CuO may act as a sintering aid as in the bulk CeO_2–ZrO_2 ceramics.[14]

Although progress has now been made in obtaining zirconia fibers with tensile strength higher than 1·0 GPa, further study on the microstructural changes caused by heating above 1000°C and the heating schedule for suppressing grain growth is needed in order to obtain fibers which can stand temperatures as high as 1400–1500°C.

5 Summary

CaO-stabilized ZrO_2 fibers have been prepared by the sol–gel method using $Zr(O\text{-}n\text{-}C_3H_7)_4$ and different CaO-sources (calcium acetate and calcium nitrate). The conversion process of gel to oxide fibers and the tensile strength of fibers were compared with one another. Then, on the basis of results for the CaO–ZrO_2 system, CeO_2–ZrO_2 fibers were fabricated. The following results were obtained.

(1) Gel fibers for the oxide composition of $11CaO.89ZrO_2$ (in mol%), 20 to 50 cm in length and ~10 to several tens μm in diameter were easily drawn by hand from the 80°C-aged $Zr(O\text{-}n\text{-}C_3H_7)_4/Ca(CH_3COO)_2$ (or $Ca(NO_3)_2$)–H_2O–C_2H_5OH–HCl solu-

tions. No important difference in spinnability was observed between alkoxide/acetate and alkoxide/nitrate solutions.

(2) The acetate groups rather covalently bonded to metal atoms in gel fibers were suddenly removed at 450°C, leaving micropores with a mean pore radius of 20–25 Å, while ionically bonded NO_3^- groups in the gel were removed gradually in the temperature range 350 to 550°C, giving rise to the formation of pores with a smaller mean radius.

(3) The tensile strength of 1000°C-treated CaO–ZrO_2 fibers was 0·7–1·0 GPa at diameters of 10–15 μm. However, the alkoxide/acetate-derived fibers decreased in strength with the increase of diameter at a faster rate than the alkoxide/nitrate-derived fibers. This was explained in terms of increased difficulty of the sudden removal of acetate groups from the fibers having increased diameters without microcrack formation.

(4) CeO_2-stabilized ZrO_2 fibers containing CeO_2 in amounts of 10 and 19 mol% were obtained using $Zr(O\text{-}n\text{-}C_3H_7)_4$ and $Ce(NO_3)_3 . 6H_2O$ as raw materials. In the latter composition, t-ZrO_2 lasted to 1400°C. The maximum tensile strength of 1·0–1·2 GPa was attained in the 1000°C-treated fibers.

(5) The addition of 1·0 mol% CuO to $19CeO_2 . 81ZrO_2$ fibers was very effective in promoting sintering of fibers, and the tensile strength of 1000°C-treated CuO-containing fibers was as high as 1·8–2·0 GPa at diameters of 10–15 μm. The strength of the fibers heated to 1100–1200°C was still as high as 0·7–0·8 GPa.

Acknowledgements

The present authors wish to thank Mr S. Sakurada of Toa Fuel Co. for the measurements of pore characteristics, and also thanks go to Professor O. Yamamoto of Faculty of Engineering, Mie University, for taking the SEM photographs.

References

1. Marshall, D. B., Lange, F. F. & Morgan, P. D., High strength zirconia fibers. *J. Am. Ceram. Soc.*, (1987) C187–C188.
2. Khavari, M. E., Lange, F. F., Smith, P. & Marshall, D. B., Continuous spinning of zirconia fibers; relations between processing and strength. *Mat. Res. Soc. Symp. Proc.*, **121** (1988) 617–21.
3. Kamiya, K. & Yoko, T., Synthesis of SiO_2 glass fibers from $Si(OC_2H_5)_4$–H_2O–C_2H_5OH–HCl solutions through sol–gel method. *J. Mat. Sci.*, **21** (1986) 842–8.
4. Kamiya, K., Tanimoto, K. & Yoko, T., Preparation of TiO_2 fibers by hydrolysis and polycondensation of $Ti(O\text{-}i\text{-}C_3H_7)_4$. *J. Mat. Sci. Lett.*, **5** (1986) 402–4.
5. Kamiya, K., Yoko, T., Tanaka, K. & Itoh, H., Preparation of fibrous ZrO_2 and CaO–ZrO_2 from zirconium alkoxide by sol–gel method. *Yogyo-Kyokai-Shi.* **95** (1987) 1157–63.
6. Kamiya, K., Yoko, T., Tanaka, K. & Itoh, H., Conversion process of gel fibers prepared from $Zr(O\text{-}n\text{-}C_3H_7)_4$ by sol–gel method to ZrO_2 fibers. In *Proc. Inter. Inst. Science and Sintering Symp.*, (*Proc. IISS Symp.*), 1988, pp. 96–101.
7. Yogo, T., Synthesis of polycrystalline zirconia fiber with organozirconium precursor. *J. Mat. Sci.*, **25** (1990) 2394–8.
8. Chatterjee, G., De, A. & Ganguli, D., Zirconia fibers from the zirconium *n*-propoxide–acethylacetone–water–isopropanol system. *J. Mat. Sci. Lett.*, **9** (1990) 845–6.
9. Sato, T. & Shimada, M., Transformation of yttria-doped tetragonal ZrO_2 polycrystals by annealing in water. *J. Am Ceram. Soc.*, **68** (1985) 356–9.
10. Tani, E., Yoshimura, M. & Somiya, S., Revised phase diagram of the system ZrO_2–CeO_2 below 1400°C. *J. Am. Ceram. Soc.*, **66** (1983) 506–10.
11. Matsumoto, R. L. K., Aging behavior of Ce-stabilized tetragonal zirconia polycrystals. *J. Am. Ceram. Soc.*, **71** (1988) C128–C129.
12. Namamoto, K., *Infrared and Raman Spectra of Inorganic and Coordination Compounds*. John Wiley & Sons, New York, 1963.
13. Doremus, R. H., Fracture and fatigue of glass. In *Treatise on Materials Science and Technology*, Vol. 22, ed. M. Tomozawa & R. H. Doremus. Academic Press, New York, 1982, pp. 178–81.
14. Mashio, M., Bischoff, E., Sbaizero, O. & Meriani, S., Sintering aids for Ce-TZP. In *Zirconia '88*, ed. S. Meriani & C. Palmorari. Elesevier Applied Science, New York, 1989, pp. 171–80.